On the Micellar Aggregates of Alkali Metal Salts of Deoxycholic Acid

Adalberto Bonincontro

INFM, Dipartimento di Fisica, Università di Roma "La Sapienza", P.le A. Moro 5, 00185 Roma, Italy

Angelo Antonio D'Archivio and Luciano Galantini

Dipartimento di Chimica, Ingegneria Chimica e Materiali, Università di L'Aquila, 67010 L'Aquila, Italy

Edoardo Giglio* and Francesco Punzo

Dipartimento di Chimica, Università di Roma "La Sapienza", P.le A. Moro 5, 00185 Roma, Italy

Received: January 22, 1999; In Final Form: April 2, 1999

The X-ray patterns of lithium (LiDC) and potassium (KDC) deoxycholate fibers, drawn from aqueous micellar solutions, have been interpreted by means of a packing of 8/1 helices formed by trimers. Previously, these helices satisfactorily represented the structure of the sodium (NaDC) and rubidium (RbDC) deoxycholate micellar aggregates. Dielectric measurements show that the trend of the average electric dipole moment μ of a NaDC monomer as a function of temperature and concentration supports a two-structure equilibrium. The high μ values (32−58 D) can be explained by the remarkable hydration of the NaDC micellar aggregates. The μ moderate decrease when the size of the aggregates increases can agree with the presence of small helices but disagrees with the existence of aggregates that are disordered or have a center (or a pseudocenter) of symmetry. Formerly, it was observed that sodium taurodeoxycholate (NaTDC) micellar aggregates, represented by 7/1 helices, formed by trimers, behave similarly. The contribution to the electrical conductivity of NaDC and NaTDC in aqueous solutions containing NaCl tends to zero by increasing the NaCl concentration, denoting strong interactions between Na^+ ions and anion aggregates. According to the similar 7/1 and 8/1 helices, which have the Na^+ ions in their inner part, the micellar size and the fraction of Na^+ ions trapped inside the helices increase together. The aggregate apparent hydrodynamic radius (R_h) increases by increasing the ionic strength in the order LiDC > NaDC > KDC > RbDC. Fibers drawn from solutions containing two cations at the same concentration show that the affinity for the anionic structure seems to follow the order $Li^+ > Na^+ > K^+ > Rb^+$ at high ionic strength. The R_h values vs the mole fractions of Li^+ and Rb^+ or Na^+ and K^+ at lower ionic strength are fitted by straight lines. Probably, the free energy gains, associated with the cation and anion transfer from the bulk solution to the micellar aggregates, are almost equal for the four salts at lower ionic strength.

Introduction

The very close X-ray diffraction patterns of sodium and rubidium deoxycholate (NaDC and RbDC, respectively) fibers were interpreted by means of similar unit cell constants and 8/1 helices, formed by trimers having a 3-fold rotation axis.[1] It is interesting to note that three molecules of the 2_1 helix, observed in a RbDC crystal[2] and satisfactorily used to explain experimental data of NaDC aqueous micellar solutions,[2−11] can easily form the trimer of the 8/1 helix.

The X-ray study of sodium (NaTDC) and rubidium taurodeoxycholate, sodium and rubidium glycodeoxycholate,[12,13] and calcium taurodeoxycholate[14] fibers showed that their structures can be represented by a packing of 7/1 helices very similar to the 8/1 helices. The 7/1 helical model was assumed for the micellar aggregates and was verified by means of some experimental techniques.[13,15,16] Moreover, electromotive force (emf) measurements, carried out on NaTDC aqueous solutions as a function of pH and ionic strength, provided the distribution of the micellar aggregation numbers (N) and revealed that each N is almost always a multiple of 3, in agreement with the 7/1 helix formed by trimers. From this distribution the mean hydrodynamic radius was calculated by means of a two-structure model formed by aggregates with an approximate shape of oblate and cylindrical objects. The good agreement between the mean hydrodynamic radius and the apparent hydrodynamic radius (R_h), obtained from quasi-elastic light-scattering (QELS) measurements for the same samples, was a further proof in favor of the 7/1 helix.[13,15] This work is devoted to the interpretation of X-ray, dielectric, conductivity, and QELS data on lithium (LiDC), sodium, potassium (KDC), and rubidium deoxycholate in order to get information on (i) the LiDC and KDC fiber structures for a comparison with those of NaDC and RbDC, (ii) the dielectric behavior of NaDC micellar solutions so as to verify the reliability of the 8/1 helical model and to compare the NaDC and NaTDC data, (iii) the NaDC and NaTDC contribution to the electrical conductivity of aqueous solutions as a function of added NaCl, and (iv) Li^+, Na^+, K^+, and Rb^+ affinity order for the anion helical structure.

Experimental Section

Materials. LiDC, KDC, and RbDC were obtained by adding to deoxycholic acid (Sigma) a little less than the equivalent amount of LiOH (Fluka, purity >99.5%), KOH (Riedel-De Haën AG, purity >86%), and RbOH aqueous solution (Aldrich) and

10.1021/jp990278h CCC: $18.00
Published on Web 05/29/1999

filtering the resulting suspension. NaDC (Calbiochem), LiDC, KDC, RbDC, and NaTDC (Sigma) were twice crystallized from a mixture of water and acetone. Glassy and brittle fibers of LiDC, NaDC, KDC, and RbDC were drawn from viscous aqueous solutions obtained by adding LiCl, NaCl, KCl, and RbCl, respectively, or HCl. LiCl, NaCl, and RbCl were from Merck (suprapur). KCl was from Fluka (purity >99.5%).

X-ray Measurements. LiDC and KDC fibers were preferentially oriented microcrystalline specimens. Their X-ray diffraction photographs were recorded on flat and cylindrical films by means of Weissenberg, Debye−Scherrer, and Buerger precession cameras, using Cu Kα and Fe Kα radiation (λ = 1.5418 and 1.9373 Å, respectively).

Dielectric Measurements. The dielectric measurements were carried out at 5, 15, 25, 35, and 45 °C on 10, 20, 30, 40, 50, 60, 70, 80, 90, and 100 mM NaDC aqueous solutions by means of an impedance analyzer HP 4291 A in the frequency range from 1.0 MHz to 1.8 GHz. The measured reflection coefficient and phase angle at the interface with the sample were converted to the real and imaginary part of the dielectric constant by an interpolation method based on dielectric measurement of electrolyte solutions that have conductivities near those of the samples investigated.[17] The dielectric loss values were obtained by subtraction of the ionic conductivity contribution according to the known formula:

$$\epsilon'' = \epsilon''_{T} - \sigma_o/(\epsilon_o\omega)$$

where ϵ" is the dielectric loss, ϵ"$_T$ is the observed imaginary part of the complex dielectric constant, σ_o is the ionic conductivity of the solution, ϵ_o is the dielectric constant in a vacuum, and ω is the angular frequency. The conductivity σ_o was measured as described in the next paragraph. The sample holder was thermostated within 0.1 °C.

Electrical Conductivity Measurements. Electrical conductivity measurements were accomplished by means of an Impedance Analyzer HP 4194 A, which covers the frequency range 10 kHz to 100 MHz. The impedance of the cell filled with the sample was measured in a narrow range of frequencies within the interval 10−100 kHz, where the phase angle is near zero, because under this condition the impedance is the electric resistance of the sample and is inversely proportional to its conductivity. It must be noted that these frequencies are so much lower than those of the solute and, even more so, of the solvent dielectric relaxation, as to exclude any contribution of dielectric loss to the measured resistance. This ensures that the ionic or static conductivity of the sample is measured. The cell constant was determined by means of measurements of standard electrolyte solutions.

QELS Measurements. A Brookhaven instrument constituted of a BI-2030AT digital correlator with 136 channels and a BI-200SM goniometer was used. The light source was an argon ion laser model 85 from Lexel Corp. operating at 514.5 nm. Dust was eliminated by means of a Brookhaven ultrafiltration unit (BIUU1) for flow-through cells, the volume of the flow cell being about 1.0 cm^3. Nuclepore filters with a pore size of 0.1 μm were used. The samples were placed in the cell and were allowed to stand 48 h prior to measurement to obtain reproducible data. Their temperature was kept constant at 25 ± 0.5 °C by a circulating water bath. The scattered intensity and the time-dependent light scattering correlation function were analyzed only at the 90° scattering angle. The observed intensity and the apparent diffusion coefficient did not depend on the exchanged wave vector in the range 30−150° in our experimental conditions. The scattering decays were analyzed by means of cumulant expansion up to second order, because higher order contributions did not improve the statistics. The apparent hydrodynamic radius was calculated by the Stokes−Einstein relationship.

TABLE 1: Observed (d_o) and Calculated (d_c) Spacings (Å) of Layer Lines for LiDC (c = 52.0 Å) and KDC (c = 51.9 Å)

	LiDC		KDC	
layer line	d_o	d_c	d_o	d_c
1	52.1	52.0	51.8	51.9
7	7.4	7.4	7.4	7.4
8	6.5	6.5	6.5	6.5
9	5.8	5.8	5.8	5.8
15	3.5	3.5	3.5	3.5

TABLE 2: Observed (d_o) and Calculated (d_c) Spacings (Å) and Miller Indices (h,k) in Parentheses of Equatorial Reflections for LiDC (a = 31.6, b = 18.2 Å) and KDC (a = 32.6, b = 18.8 Å)

LiDC		KDC	
d_o	d_c (h,k)	d_o	d_c (h,k)
10.6	10.5 (3,0)	32.6	32.6 (1,0)
9.0	9.1 (0,2) (3,1)	16.3	16.3 (1,1) (2,0)
8.7	8.7 (1,2)	12.3	12.3 (2,1)
7.9	7.9 (4,0) (2,2)	10.9	10.9 (3,0)
6.9	6.9 (3,2)	9.4	9.4 (0,2) (3,1)
6.0	6.0 (1,3) (4,2) (5,1)	9.0	9.0 (1,2)
5.7	5.7 (2,3)	8.2	8.2 (4,0) (2,2)
		6.2	6.2 (1,3) (4,2) (5,1)

Results

X-ray Study of LiDC and KDC Fibers. The X-ray diffraction photographs of LiDC and KDC air-dried fibers show the most intense layer lines clearly resolved into a series of spots. Their intensity distribution is typical of helical structures. The alkali halides interplanar spacings, known with great precision, have been used to determine those of LiDC and KDC. The observed spacings of the most intense LiDC and KDC layer lines and equatorial reflections are listed in Tables 1 and 2, respectively. The LiDC and KDC equatorial reflections can be indexed in a two-dimensional lattice with the rectangular cell constants a = 31.6 Å and b = 18.2 Å (LiDC) and a = 32.6 Å and b = 18.8 Å (KDC). Each unit cell contains two helices with a radius of about 9.1 Å (LiDC) and 9.4 Å (KDC), assuming that the helices are closely packed cylinders.

A group of three intense layer lines near the meridian (seventh, eighth and ninth layer line) show spacings of about 7.4, 6.5, and 5.8 Å. The eighth layer line is the most intense and, hence, its spacing could correspond to the helical axis projection of the distance between two consecutive equivalent points on the helix that has eight (or nearly eight) points in the identity period. The helical transform theory,[18] applied to LiDC and KDC, supports the 8/1 helix, which presents appreciable intensity observed only for layer lines characterized by zero or near zero values of the permitted orders of Bessel functions. The comparison of the estimated average intensity of each layer line with the permitted orders of Bessel functions is equal to that previously published for NaDC and RbDC (see Table 3 of ref 1).

Dielectric and Electrical Conductivity Studies. The complex dielectric constant $\epsilon^* = \epsilon' - j\epsilon''$ of NaDC aqueous solutions has been measured as a function of frequency. As an example, the permittivity ϵ' and the dielectric loss ϵ'' of the 100 mM NaDC solution are shown vs frequency at different temperatures in Figures 1 and 2, respectively. The experimental point trends reveal the presence of the dielectric relaxation

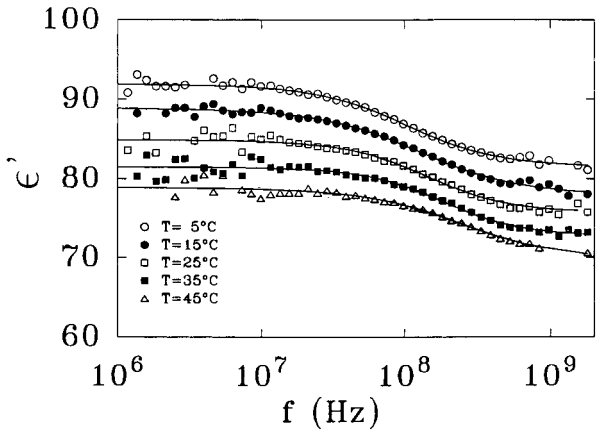

Figure 1. Permittivity of the 100 mM NaDC aqueous solution vs frequency at different temperatures.

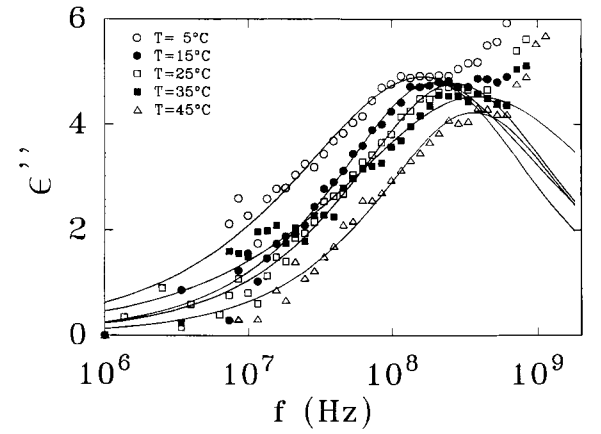

Figure 2. Dielectric loss of the 100 mM NaDC aqueous solution vs frequency at different temperatures.

usually observed in macromolecular solutions at these frequencies.[19−22] The full lines represent the best fit in terms of a Cole−Cole dispersion applying the known equation:

$$\epsilon^* = \epsilon_\infty + \Delta\epsilon/[1 + (j\omega\tau)^{1-\alpha}]$$

where ϵ_∞ is the high-frequency limit permittivity, $\Delta\epsilon$ is the dielectric increment, τ is the relaxation time, and α is an empirical parameter that indicates a spread of relaxation times. Because the relaxation frequency of water varies from 10 to 20 GHz within the temperature range 5−25 °C, its contribution to the dielectric loss is becoming appreciable near 1 GHz, especially for the lower temperatures (Figure 2). The Oncley formula,[23,24] verified in solutions with solutes of molecular weights comparable with those of the NaDC micellar aggregates,[1,3,25−29] permits evaluation of the apparent electric dipole moment of the solute from the dielectric increment:

$$\mu^2 = 2kT\epsilon_o M\Delta\epsilon/N_o c$$

where μ is the "effective" electric dipole moment, k is the Boltzmann constant, T is the absolute temperature, M is the molecular weight of the NaDC monomer, N_o is the Avogadro number, and c is the solute concentration in g m^{-3}. This relationship assumes that the dielectric relaxation is due to orientational polarizability of polar molecules or assemblies of molecules in solution. The "effective" μ value is calculated in the limit of noninteracting micellar aggregates[28] for the NaDC monomer and not for the micellar aggregates (M refers to the monomer) and represents the average electric dipole moment of the NaDC monomer in its specific aggregation distribution function of the solution. The μ values, estimated by the Oncley formula, are depicted as a function of NaDC concentration in Figure 3. The μ values are practically constant in the temperature range 15−45 °C at a fixed concentration. As an example, the data of the 10 and 100 mM samples are shown in Figure 4.

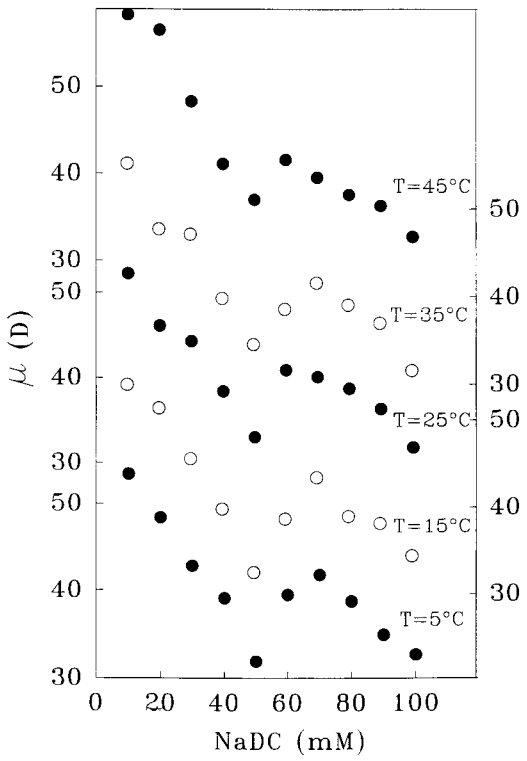

Figure 3. Average electric dipole moment per NaDC monomer as a function of NaDC concentration at different temperatures. The left and right scale are for the black and open circles, respectively.

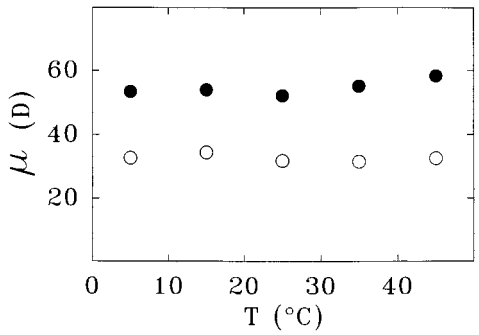

Figure 4. Average electric dipole moment per NaDC monomer as a function of temperature. Black and open circles refer to the 10 and 100 mM sample, respectively.

To get information on the location of the cations belonging to the 8/1 and 7/1 helices and on the nature of their interaction with the anions, electrical conductivity measurements have been performed on 0.1 M NaDC, KDC, and NaTDC aqueous solutions at 25 °C as a function of added NaCl or KCl (Figure 5). The NaDC and NaTDC experimental points are practically superimposed.

QELS Study of LiDC, NaDC, KDC, and RbDC Aqueous Solutions. The R_h values of 0.1 M LiDC, NaDC, KDC, and RbDC aqueous solutions are shown as a function of MCl (M = Li, Na, K, or Rb) concentration of the corresponding chloride in Figure 6. They are rather equal up to 300 mM MCl and follow

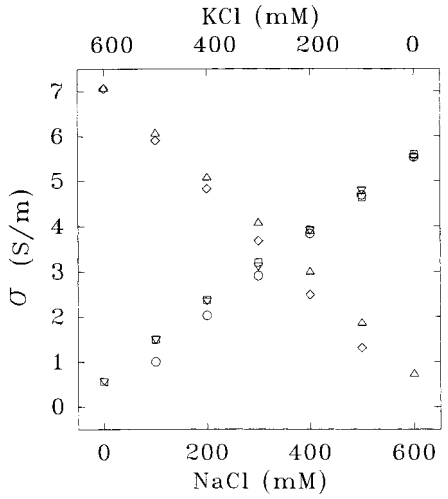

Figure 5. Specific conductivity of NaDC + NaCl (squares), NaTDC + NaCl (up-pointing triangles), and KDC + KCl (down-pointing triangles) as a function of added NaCl or KCl. Those of NaCl (circles) and KCl (diamonds) are shown for comparison. The NaDC, NaTDC, and KDC concentration is 100 mM. The upper abscissa refers to KDC + KCl and KCl.

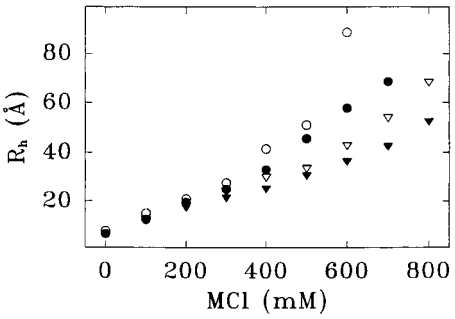

Figure 6. R_h of 0.1 M LiDC (open circles), NaDC (black circles), KDC (open triangles), and RbDC (black triangles) aqueous solutions as a function of LiCl, NaCl, KCl, and RbCl concentration, respectively (M = Li, Na, K, or Rb). The average standard deviation is ±0.3 Å.

the order LiDC > NaDC > KDC > RbDC at higher concentrations. Moreover, QELS measurements have been accomplished to get information on the relative affinity of the cations for the anion aggregates at ionic strengths, which are lower than those of fibers formation. Aqueous solutions containing deoxycholate anions (100 mM) and LiCl + RbCl or NaCl + KCl in such a way as to keep constant $Li^+ + Rb^+$ (500 mM) or $Na^+ + K^+$ (600 mM) concentration have been investigated. The plots of R_h against Li^+ or Na^+ concentration are shown in Figure 7.

Discussion

The spacings and the estimated average intensities of the layer lines from 1 to 15 are practically equal for LiDC and KDC as well as for NaDC and RbDC and correspond to identity periods along the helical axis of 52.0 Å (LiDC), 51.9 Å (KDC), 52.0 Å (NaDC),[1] and 51.6 Å (RbDC).[1] The LiDC and KDC rectangular cell constants are very close to those of NaDC (a = 32.3 Å and b = 18.7 Å) and RbDC (a = 34.1 Å and b = 19.7 Å).[1] The LiDC, NaDC, KDC, and RbDC packings are all trigonal or hexagonal.[1] Therefore, the 8/1 helical structure is common to the LiDC, NaDC, KDC, and RbDC fibers and, very likely, represents that of the micellar aggregates. The polar heads approach the helical axis as in the case of the 7/1 helix, and hence, cations are reasonably located in the interior of the helix.[1,13] This hypothesis is supported by the increase of the

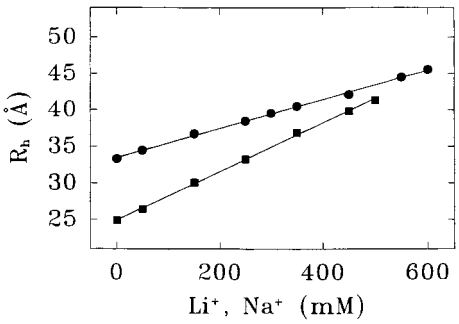

Figure 7. R_h of aqueous solutions containing deoxycholate anions (100 mM) and $Li^+ + Rb^+$ ions (500 mM) (black squares) or $Na^+ + K^+$ ions (600 mM) (black circles) as a function of Li^+ or Na^+ concentration, respectively. The average standard deviation is ±0.3 Å.

helical radius in the order LiDC < NaDC < KDC < RbDC (9.1, 9.3_5, 9.4, and 9.8_5 Å, respectively),[1] since the hydrated cation volume in the solid state increases in the same order. On the other hand, the structures of the 8/1 and 7/1 helices display similar characteristics. They have repetitive units formed by similar trimers, nearly equal translations of the repetitive unit along the helical axis (6.4−6.5 Å), and close rotations of the repetitive unit around the helical axis (45.0° for the 8/1 helix and 34.3° for the 7/1 helix). Both the helices are mainly polar inside and apolar outside and are stabilized chiefly by similar polar interactions.[1,13] Thus, if the NaDC and NaTDC micellar aggregates possess the 8/1 and 7/1 helical structures, respectively, their properties should be very alike.

The NaDC μ values decrease from 58 to 32 D (from 68 to 33 D in the case of NaTDC[15]) when concentration increases from 10 to 100 mM. They, considered as average values of single NaDC molecules belonging to the aggregates, seem too high. Since the distances between Na^+ and the oxygen atoms of the carboxylate groups vary approximately between 2.2 and 4.5 Å as, for example, in the crystal structures of sodium glycodeoxycholate[8] and glycocholate,[30] a realistic estimate does not exceed ∼20 D. However, the high μ values could be justified by a contribution of the hydration water, because, for instance, the cation hydration is supported by extended X-ray absorption fine structure measurements of RbDC aqueous micellar solutions, which indicate that the Rb^+ ions are coordinated to 8−9 oxygen atoms in the first shell having a radius of about 3.8 Å.[4] In fact, the cations, the aggregates (especially the polar heads), and their coordinated water molecules can move and can be oriented by applying an electric field.

The experimental points at all the investigated temperatures can be fitted by a straight line within the concentration range 10−50 mM. At this last value μ presents a minimum followed by a maximum at a concentration 60−70 mM, and from this maximum up to 100 mM the trend is approximately linear (Figure 3). Dielectric measurements allowed the average electric dipole moment μ of a NaTDC monomer to be calculated as a function of NaTDC concentration (10−100 mM) and temperature (5−45 °C). The μ data of NaTDC, which can be fitted by two straight lines intersecting at a concentration about 40−50 mM, were explained by resorting to the hypothesis of the coexistence of two structures, one prevailing in the range 10 to ∼40 mM and the other in the range ∼50−100 mM.[13,15] The first structure has $N \leq 12$ (from one to four trimers) and an approximate shape of oblate ellipsoid formed by trimers with NaTDC molecules approximately in the fully extended conformation (semimajor axis of ∼22 Å). The second structure has $N \geq 15$ (from five trimers upward) and an approximate cylindrical shape (that of the 7/1 helix, which has a radius of ∼10.2 Å),

since it was reasonably supposed that the cooperative effect in the formation of the 7/1 helix arises starting from the pentadecamer. In fact, the strongest interactions in the 7/1 helix are those between a trimer j and the trimers $j \pm 1$ and $j \pm 2$, and the smallest aggregate, which give rise to all four of these interactions is the pentadecamer.[13] Also, NaDC can behave likewise, owing to the very close geometries of the 8/1 and 7/1 helices. The model of the 8/1 helix for NaDC is validated also by the trimers observed in the NaDC aqueous micellar solutions by means of emf measurements, especially at low ionic strength.[25] Therefore, the μ data of NaDC can be interpreted as those of NaTDC by a two-structure model, assuming that the oblate and the cylindrical aggregates prevail in concentration ranges 10−50 mM and ∼60 or 70−100 mM, respectively. The moderate decrease of μ in these ranges by increasing the NaDC concentration and micellar size agrees with the growth of helical aggregates and permits us to discard models that are disordered or have a center or pseudocenter of symmetry. The increase of μ in the concentration region from 50 to 60−70 mM could be explained by assuming that in this region the smallest cylindrical aggregates begin to form and their μ is greater than that of the oblate aggregates that are present in the same region.

The nearly constant μ values in the temperature range 15−45 °C at a fixed concentration seem to indicate no remarkable change in the structure and size of the aggregates within that range and points out that their structure is stable. Moreover, it must be noticed that the dielectric results refer to solutions without NaCl, containing aggregates of small size.

The contribution to conductivity of NaDC and NaTDC cations and anions (monomers and aggregates) is nearly equal, thus confirming a close interaction energy between Na^+ ions and anionic aggregates in the very similar 8/1 and 7/1 helices. The conductivity difference of NaCl aqueous solutions with or without 0.1 M NaDC (or NaTDC) decreases by increasing the NaCl concentration, being practically zero from 400 to 600 mM (Figure 5). Within this range it seems that only NaCl conducts and NaDC (or NaTDC) gives no contribution. On the other hand, within this range their micellar sizes vary, and hence, the obstruction effect of the aggregates seems to be negligible. These results suggest that the Na^+ ion percentage, progressively trapped inside the anion aggregates, increases up to 400 mM NaCl concentration and afterward remains approximately constant. As a consequence, Na^+ ions strongly interact by means of polar forces with the anion aggregates, and their fractional binding is very high, in accordance with the emf NaDC[25] and NaTDC[13,16] data.

An almost similar situation is observed in the case of KDC. However, the conductivity difference of KCl aqueous solutions with or without 0.1 M KDC is nearly zero only at 600 mM KCl concentration. Specific conductivity data of LiDC, NaDC, KDC, and RbDC aqueous solutions (pH ∼6.8−6.9) recorded as a function of temperature[31] support this result. At this pH salts are near the gelation point, so that their aggregates are large and have the 8/1 helical structure observed in the fibers, which are drawn from these solutions by means of a moderate elongational stress.[1] The break in the linear trend, corresponding to a particular temperature (transitional temperature), reveals a structural transition that depends on the cation. Because the slope after the break (higher temperatures) is greater than that at lower temperatures, it is reasonable to suppose a greater number of cations are released from micellar aggregates, which, very probably, decrease the aggregate's size. The transitional temperature, as well as the micellar aggregate thermal stability, increases with the decreasing cation crystallographic radius and follows the order LiDC > NaDC > KDC > RbDC.[31] Of course, a shorter crystallographic radius implies shorter distances between the cation and, for instance, the polar head oxygen atoms, and stronger polar interactions. Furthermore, the cation charge density decreases in the order $Li^+ > Na^+ > K^+ > Rb^+$. Therefore, Na^+ ions are more firmly anchored to the anion structure than K^+ ions, and KDC micellar size equals that of NaDC at higher ionic strength (Figure 6).

The data of Figure 6 suggest that at high ionic strength the micellar size decreases in the order LiDC > NaDC > KDC > RbDC and the affinity for the anion helical structure is $Li^+ > Na^+ > K^+ > Rb^+$, even though micellar growth can be affected by factors as, for instance, the medium dielectric constant, which depends on the added alkali chloride. To validate this scale, fibers have been drawn from aqueous solutions containing (a) LiDC, NaDC, LiCl, and NaCl, (b) LiDC, KDC, LiCl, and KCl, (c) LiDC, RbDC, LiCl, and RbCl, (d) NaDC, KDC, NaCl, and KCl, (e) NaDC, RbDC, NaCl, and RbCl, and (f) KDC, RbDC, KCl, and RbCl, the initial concentration of each compound being 200 mM. X-ray patterns have shown that samples a−f, under the condition of high ionic strength, give rise to LiDC fibers and NaCl crystals, LiDC fibers and KCl crystals, LiDC fibers and RbCl crystals, NaDC fibers and KCl crystals, NaDC fibers and RbCl crystals, and KDC fibers and $K_xRb_{1-x}Cl$ crystals, respectively. These results agree with the affinity scale, since fibers are composed of helices already present in the aqueous solutions and in the gel phases. It is worth emphasizing that the crystals grow by evaporation of the mother liquor on the surface of the fibers previously formed.

Finally, the observed linear trends of Figure 7 are characteristic of free energy gains, associated with cation and anion transfer from the bulk solution to the micellar aggregates, that are nearly equal for the two cations of each pair. Thus, cation affinities for the anion helical structure tend to equalize by decreasing ionic strength, in agreement with trends of Figure 6.

Acknowledgment. This work was sponsored by the Italian Ministero per l'Università e per la Ricerca Scientifica e Tecnologica (Cofin. MURST 97 CFSIB) and by the Istituto Nazionale di Fisica della Materia.

Supporting Information Available: One table detailing the dielectric data of NaDC aqueous solutions at different temperatures. The relaxation frequency f_0 and the dielectric increment $\Delta\epsilon$ are reported. This material is available free of charge via the Internet at http://pubs.acs.org.

References and Notes

(1) D'Archivio, A. A.; Galantini, L.; Giglio, E.; Jover, A. *Langmuir* **1998,** *14*, 4776.
(2) Campanelli, A. R.; Candeloro De Sanctis, S.; Giglio, E.; Petriconi, S. *Acta Crystallogr., Sect. C* **1984**, *C40*, 631.
(3) Esposito, G.; Giglio, E.; Pavel, N. V.; Zanobi, A. *J. Phys. Chem.* **1987**, *91*, 356.
(4) Giglio, E.; Loreti, S.; Pavel, N. V. *J. Phys. Chem.* **1988**, *92*, 2858.
(5) Conte, G.; Di Blasi, R.; Giglio, E.; Parretta, A.; Pavel, N. V. *J. Phys. Chem.* **1984**, *88*, 5720.
(6) D'Alagni, M.; Forcellese, M. L.; Giglio, E. *Colloid Polym. Sci.* **1985**, *263*, 160.
(7) Esposito, G.; Zanobi, A.; Giglio, E.; Pavel, N. V.; Campbell, I. D. *J. Phys. Chem.* **1987**, *91*, 83.
(8) Campanelli, A. R.; Candeloro De Sanctis, S.; Chiessi, E.; D'Alagni, M.; Giglio, E.; Scaramuzza, L. *J. Phys. Chem.* **1989**, *93*, 1536.
(9) Burattini, E.; D'Angelo, P.; Giglio, E.; Pavel, N. V. *J. Phys. Chem.* **1991**, *95*, 7880.
(10) Chiessi, E.; D'Alagni, M.; Esposito, G.; Giglio, E. *J. Inclusion Phenom. Mol. Recognit. Chem.* **1991**, *10*, 453.
(11) D'Alagni, M.; Delfini, M.; Galantini, L.; Giglio, E. *J. Phys. Chem.* **1992**, *96*, 10520.

(12) D'Alagni, M.; D'Archivio, A. A.; Giglio, E.; Scaramuzza, L. *J. Phys. Chem.* **1994**, *98*, 343.
(13) Briganti, G.; D'Archivio, A. A.; Galantini, L.; Giglio, E. *Langmuir* **1996**, *12*, 1180.
(14) D'Archivio, A. A.; Galantini, L.; Giglio, E. *Langmuir* **1997**, *13*, 4197.
(15) Bonincontro, A.; Briganti, G.; D'Archivio, A. A.; Galantini, L.; Giglio, E. *J. Phys. Chem.* **1997**, *101*, 10303.
(16) Bottari, E.; Festa, M. R. *Langmuir* **1996**, *12*, 1777.
(17) Athey, T. W.; Stuchly, M. A.; Stuchly, S. S. *IEEE* **1982**, *MTT 30*, 82.
(18) Cochran, W.; Crick, F. H. C.; Vand, V. *Acta Crystallogr.* **1952**, *5*, 581.
(19) Shepherd, J. C.; Grant, E. H. *Proc. R. Soc. London* **1968**, *A307*, 335.
(20) Takashima, S.; Gabriel, C.; Sheppard, R. J.; Grant, E. H. *Biophys. J.* **1984**, *46*, 29.
(21) Bonincontro, A.; Caneva, R.; Pedone, F. *J. Non-Cryst. Solids* **1991**, *133*, 1186.
(22) Pedone, F.; Bonincontro, A. *Biochim. Biophys. Acta* **1991**, *1073*, 580.
(23) Oncley, J. L. In *Proteins, Amino Acids and Peptides*; Cohn, E. J., Edsall, J. T., Eds.; Reinhold: New York, 1943; p 543.
(24) Pethig, R.; Kell, D. B. *Phys. Med. Biol.* **1987**, *32*, 933.
(25) Bottari, E.; Festa, M. R.; Jasionowska, R. *J. Inclusion Phenom. Mol. Recognit. Chem.* **1989**, *7*, 443.
(26) Takashima, S. In *Physical Principles and Techniques of Protein Chemistry, Part A*; Leach, A. J., Ed.; Academic: New York, 1969; p 291.
(27) Gerber, B. R.; Routledge, L. M.; Takashima, S. *J. Mol. Biol.* **1972**, *71*, 317.
(28) Grant, E. H.; Sheppard, R. J.; South, G. P. In *Dielectric Behaviour of Biological Molecules in Solution*; Clarendon: Oxford, U.K., 1978.
(29) Pethig, R. In *Dielectric and Electronic Properties of Biological Materials*; Wiley: Chichester, U.K., 1979.
(30) Campanelli, A. R.; Candeloro De Sanctis, S.; Galantini, L.; Giglio, E. *J. Inclusion Phenom. Mol. Recognit. Chem.* **1991**, *10*, 367.
(31) Botré, C.; Cicconetti, P. A.; Lionetti, G.; Marchetti, M. *J. Pharm. Sci.* **1967**, *56*, 1035.